Engineering Transactions, **72**(1): 81–94, 2024, doi: 10.24423/EngTrans.3116.2024
Institute of Fundamental Technological Research Polish Academy of Sciences (IPPT PAN)
Université de Lorraine • Poznan University of Technology

Research Paper

The Saint-Venant Torsion of a Cartesian Orthotropic Bar With an Isosceles Right-Angled Triangle Cross-Section

István ECSEDI, Attila BAKSA*

Institute of Applied Mechanics, University of Miskolc
Miskolc Egyetemváros, Hungary H-5315

** Corresponding Author e-mail: attila.baksa@uni-miskolc.hu*

The Saint-Venant torsion of the Cartesian orthotropic homogeneous linearly elastic bar is considered. The cross-section of the prismatic bar is an isosceles right-angled triangular plane domain. An approximate analytical method is presented to obtain Prandtl's stress function, shearing stresses, and torsional rigidity. Upper and lower bounds for the torsional rigidity are provided. The obtained results for shearing stresses are verified through FEM computation.

Keywords: Saint-Venant torsion; approximate analytical solution; lower and upper bounds; torsional rigidity; orthotropic.

1. Introduction

The Saint-Venant torsion of homogeneous Cartesian orthotropic linearly elastic bars has been extensively studied from both theoretical and numerical perspectives. The Saint-Venant torsion problem refers to the torsional deformation of an isotropic elastic bar. It is a classical problem in the field of solid mechanics and structural engineering. Here are the key assumptions:

a) the material is isotropic,
b) the bar is prismatic,
c) the deformation is small enough to remain within the elastic range.

The rate of twist or the twist angle ϑ can be determined by solving the differential equation that describes the torsional deformation. Using the Saint-Venant torsion theory allows for the analysis of the torsional behavior of non-circular cross-sections. For special cross-sections, such as those with complex geometry, the application of Saint-Venant's theory can be challenging, and alternative methods or modifications have been proposed.

Torsion of non-circular bars (applying Saint-Venant's theory of torsion) is well described, e.g., in book by Jog [1]. The problem is defined in detail, and

analytical solutions are presented for some isotropic and homogenous cross-sections, such as, elliptical, triangular, rectangular, circular cut in a circular cross-section, annular sector, cardioid section, and hollow beams are also discussed [2–5].

Nevertheless, there are several challenges with special cross-sections:

a) with irregular shapes or discontinuities, the assumptions of Saint-Venant's theory may not hold true in proximity to the applied torque,
b) stress concentrations and localized effects can occur in certain areas of the cross-section.

The relevant developments in torsion theory spanned the 19th and early 20th centuries, with contributions from Cauchy, Saint-Venant, and others. The specific timeline of developments can vary based on the aspects of the theory and the cross-sections considered.

Numerous books [2, 6–10, 13, 14] give in-depth analyses of the problem of uniform torsion in Cartesian orthotropic bars. Ecsedi and Baksa [12] provided a solution for the uniform torsion of an orthotropic bar with solid cross-section through a suitable coordinate transformation. The Saint-Venant torsion of the orthotropic bar in [12] is simplified to the solution of the torsion problem of the isotropic bar. Chen and Wei [17] studied the Saint-Venant torsion of Cartesian anisotropic bars with affine transformation. The non-warping property of twisted anisotropic cross-sections is discussed in papers [10, 11, 17–20]. In [15], two inequality relations are proven for the torsional rigidity of the Cartesian orthotropic solid cross-section. The presented bounding formulae for torsional rigidity are based on mean value theorems in integral calculus [15]. Swider *et al.* [16] proposed an original method to investigate the Saint-Venant torsion of anisotropic cross-section. The method employing an energy approach was used to calculate the Prandtl's stress function, represented by an infinite series of trigonometric functions. The method is illustrated in a bar with a rectangular cross-section [16]. Nowinski [21] derived bounds for the torsional rigidity of anisotropic bars with one plane of elastic symmetry perpendicular to the axis of the bar. The proof of bounding formulae of torsional rigidity is based on the Cauchy-Schwartz inequality. The lower bound is obtained by formulating the problem in terms of Prandtl's stress function, while the upper bound is derived from the formulation of the torsional function paper [21].

This paper deals with an approximate analytical solution for the uniform torsion of an orthotropic bar whose cross-section is an isosceles right-angled triangle. The complementary energy method of linear elasticity is employed to derive the approximate analytical solution for the considered uniform torsional problem. It must be noted that one of the orthotropy axes is parallel to the symmetry axis of the cross-section (Fig. 1).

Modern computational methods, such as finite element analysis (FEA), allow engineers to more accurately analyze torsion in structures with arbitrary cross-sections. FEA takes into account the full three-dimensional geometry and material properties, providing a more detailed understanding of the torsional behavior. The obtained results for shearing stresses are validated by finite element computations for the accuracy of shearing stresses and torsional rigidity.

2. Governing equations

The cross-section of the considered bar is shown in Fig. 1. The shear moduli of the bar are $G_x = G_{xz}$, $G_y = G_{yz}$.

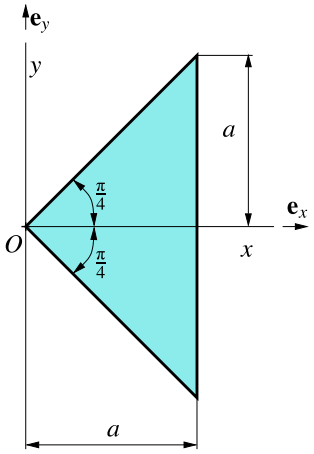

Fig. 1. The cross-section of the Cartesian orthotropic homogeneous bar.

The solution of the Saint-Venant torsion problem for the orthotropic cross-section can be obtained as a solution to the following variational problem:

$$\Pi\left[U(x,y)\right] \geq \Pi\left[\widetilde{U}(x,y)\right], \tag{2.1}$$

where $\widetilde{U} = \widetilde{U}(x,y)$ denotes an arbitrary statically admissible stress function that satisfies the homogeneous boundary condition on the curve ∂A of the solid cross-section A:

$$\widetilde{U}(x,y) = 0, \qquad (x,y) \in \partial A, \tag{2.2}$$

and the explicit form of $\Pi\left[\widetilde{U}(x,y)\right]$ is as follows:

$$\Pi\left[\widetilde{U}(x,y)\right] = 4\int\limits_A \widetilde{U}(x,y)\,\mathrm{d}A - \int\limits_A \left[\frac{1}{G_y}\left(\frac{\partial \widetilde{U}}{\partial x}\right)^2 + \frac{1}{G_x}\left(\frac{\partial \widetilde{U}}{\partial y}\right)^2\right]\mathrm{d}A. \tag{2.3}$$

Furthermore, $U = U(x, y)$ is the solution to the boundary value problem defined by Eqs. (2.4) and (2.5):

$$\frac{1}{G_y}\frac{\partial^2 U}{\partial x^2} + \frac{1}{G_x}\frac{\partial^2 U}{\partial y^2} = -2, \qquad (x, y) \in A, \tag{2.4}$$

$$U(x, y) = 0, \qquad (x, y) \in \partial A. \tag{2.5}$$

The torsional rigidity S of the cross-section A is defined as:

$$S = \frac{T}{\vartheta}, \tag{2.6}$$

where T is the applied torque. and ϑ is the rate of twist. The following formulae are valid for S:

$$\begin{gathered} S = 2\int\limits_A U \,\mathrm{d}A, \qquad S = \Pi\left[U(x, y)\right], \\ S = \int\limits_A \left[\frac{1}{G_y}\left(\frac{\partial U}{\partial x}\right)^2 + \frac{1}{G_x}\left(\frac{\partial U}{\partial y}\right)^2\right] \mathrm{d}A. \end{gathered} \tag{2.7}$$

The presented analytical method is based on Eq. (2.1), providing an approximate solution to the torsional problem. It always yields a lower bound for the exact value of the torsional rigidity.

The expressions for shearing stresses τ_{xz} and τ_{yz} in terms of the Prandtl stress function $U = U(x, y)$ are as follows:

$$\tau_{xz}(x, y) = \vartheta\frac{\partial U}{\partial y}, \qquad \tau_{yz}(x, y) = -\vartheta\frac{\partial U}{\partial x}. \tag{2.8}$$

3. Approximate analytical solution

The solution to the variational problem formulated in Eq. (2.1) is sought as:

$$\widetilde{U}(x, y) = F(x)(y^2 - x^2), \qquad (x, y) \in A \cup \partial A, \tag{3.1}$$

where the function $F = F(x)$ satisfies the following boundary conditions (see Fig. 1):

$$F(a) = 0, \qquad \lim_{x \to a} F(x) = 0. \tag{3.2}$$

The analytical approximation of the Prandtl stress function is obtained based on calculating the function $F = F(x)$ that maximizes the right-hand side of inequality (2.1). Inserting the expression for the statically admissible stress function $\widetilde{U} = \widetilde{U}(x, y)$ into the inequality, relation (2.3) gives:

$$\Pi[F(x)] = \int_0^a \left[-\frac{16}{3}x^3 F(x) - \frac{2}{5}\frac{x^5}{G_y}\left(\frac{\mathrm{d}F}{\mathrm{d}x}\right)^2 + \frac{4}{3G_y}x^3\frac{\mathrm{d}F}{\mathrm{d}x}\left(-x^2\frac{\mathrm{d}F}{\mathrm{d}x} - 2xF(x)\right)\right]\mathrm{d}x + \int_0^a \left[\frac{2}{G_y}\left(-x^2\frac{\mathrm{d}F}{\mathrm{d}x} - 2xF(x)\right)^2 - \frac{8}{3G_x}x^3\right]\mathrm{d}x. \tag{3.3}$$

The stationary condition of the functional (3.3) under the boundary condition (3.2) yields a second-order ordinary differential equation for $F = F(x)$:

$$-G_x x^2\frac{\mathrm{d}^2F}{\mathrm{d}x^2} - 5xG_x\frac{\mathrm{d}F}{\mathrm{d}x} - \frac{5}{2}G_xF + \frac{5}{2}G_yF + \frac{5}{2}G_xG_y = 0, \qquad 0 < x < a. \tag{3.4}$$

The solution to the differential Eq. (3.4), which is bounded at $x = 0$ and $F(a) = 0$, can be represented for $G_x \neq G_y$ as:

$$F(x) = cx^\lambda + \frac{G_xG_y}{G_x - G_y}, \qquad 0 \leq x \leq a, \tag{3.5}$$

$$\lambda = -2G_x + \sqrt{1.5G_x^2 + 2.5G_xG_y}, \qquad c = -\frac{G_xG_y}{a^\lambda(G_x - G_y)}. \tag{3.6}$$

The approximate expression for the Prandtl stress function is given by the following equation:

$$\widetilde{U}(x, y) = \left(cx^\lambda + \frac{G_xG_y}{G_x - G_y}\right)(y^2 - x^2), \quad (x, y) \in A \cup \partial A, \quad G_x \neq G_y. \tag{3.7}$$

The contour lines of $\widetilde{U} = \widetilde{U}(x, y)$ are shown in Fig. 2, using the following material and geometric data: $G_x = 7.5 \cdot 10^8$ Pa, $G_y = 15 \cdot 10^8$ Pa, $a = 0.45$ m.

The approximate value of the torsional rigidity can be calculated according to Eq. (2.7).

$$S_L = \frac{2}{3}a^4\frac{G_xG_y\left(4G_x - \sqrt{2G_x\left(3G_x + 5G_y\right)}\right)}{\left(G_x - G_y\right)\left(4G_x + \sqrt{2G_x\left(3G_x + 5G_y\right)}\right)} < S. \tag{3.8}$$

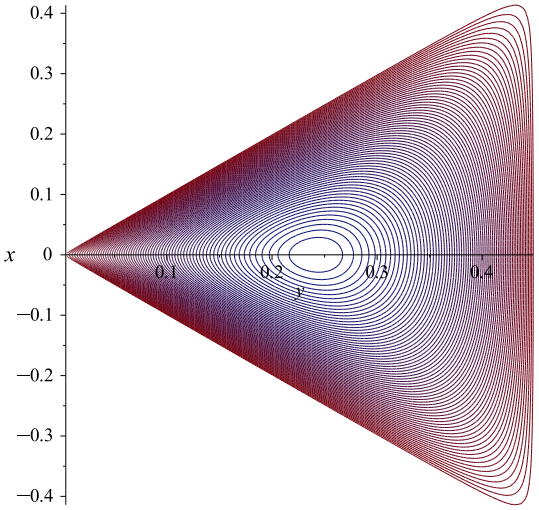

FIG. 2. Plots of the contour lines of the Prandtl stress function.

The approximate numerical value of the torsional rigidity for the data used above in Fig. 2 is as follows: $S_L = 4.95291486 \cdot 10^6\ \mathrm{N \cdot m^2}$ It must be noted that S_L given by formula (3.8) is a lower bound for the true value of the torsional rigidity according to the inequality (2.1). The following upper bound can be derived for S using Nowinski's paper [21]:

$$S \leq S_U = \int_A \left(G_x y^2 + G_y x^2\right) \mathrm{d}A - \frac{\left(\int_A \left(G_x \frac{\partial \omega}{\partial x} y - G_y \frac{\partial \omega}{\partial y} x\right) \mathrm{d}A\right)^2}{\int_A \left(G_x \left(\frac{\partial \omega}{\partial x}\right)^2 + G_y \left(\frac{\partial \omega}{\partial y}\right)^2\right) \mathrm{d}A}, \tag{3.9}$$

where $\omega = \omega(x, y)$ is a non-constant function whose first-order partial derivatives are continuous functions of x and y. Function $\omega = \omega(x, y)$ is called a kinematically admissible torsion function; otherwise, it is an arbitrary non-zero function [1, 22]. Substituting for $\omega = \omega(x, y)$ the following functions

$$\omega(x, y) = -12xya + 9x^2 y - y^3, \qquad (x, y) \in A \cup \partial A, \tag{3.10}$$

gives

$$S \leq S_U = \frac{1}{30} \left(3G_x + G_y\right) a^4. \tag{3.11}$$

In the inequality relation (3.9), the equality is reached only if $\omega(x, y) = c\phi(x, y)$, where $\phi = \phi(x, y)$ is the torsion function of the considered cross-section, and c is an arbitrary constant different from zero.

The numerical value of the upper bound for the torsional rigidity with the following data: $G_x = 7.5 \cdot 10^8$ Pa, $G_y = 15 \cdot 10^8$ Pa, $a = 0.45$ m is $S_U = 5.12578125 \cdot 10^6$ N $\cdot$ m^2. In this example, the true value of the torsional rigidity S can be estimated by application of the following two-sided bounds:

$$4.95291486 \cdot 10^6 \text{ N} \cdot \text{m}^2 \leq S \leq 5.12478125 \cdot 10^6 \text{ N} \cdot \text{m}^2. \tag{3.12}$$

The approximate formulae for shearing stresses can be obtained according to Eq. (2.8):

$$\tau_{xz}(x,y) = 2\vartheta \left(cx^{\lambda+1} + \frac{G_x G_y}{G_x - G_y} \right) y, \quad G_x \neq G_y, \tag{3.13}$$

$$\tau_{yz}(x,y) = \vartheta \left(2cx^{\lambda+1} + \frac{2G_x G_y}{G_x - G_y} x - c\lambda x^{\lambda-1}(y^2 - x^2) \right), \quad G_x \neq G_y. \tag{3.14}$$

4. The effect of the shear moduli on the solution of the torsion problem

In this section, the effect of the ratio of shear moduli on the solution of the Saint-Venant torsional problem is discussed. The results are illustrated with numerical examples. The following data are used:

$$a = 0.45 \text{ m}, \qquad G_x = 7.5 \cdot 10^8 \text{ Pa}, \qquad G_y = pG_x, \qquad \vartheta = 0.14 \text{ rad/m}. \tag{4.1}$$

The shearing stresses and torsional rigidity depend on the parameter $p > 1$, and this fact is emphasized by the following designations: $\tau_{xz}(x,y,p)$, $\tau_{yz}(x,y,p)$, $S_L(p)$, $S_U(p)$. Figure 3 shows the plots of shearing stresses $\tau_{yz}(x,0,p)$ for five different values of p ($p = 1.1$, 1.5, 2, 3, 4).

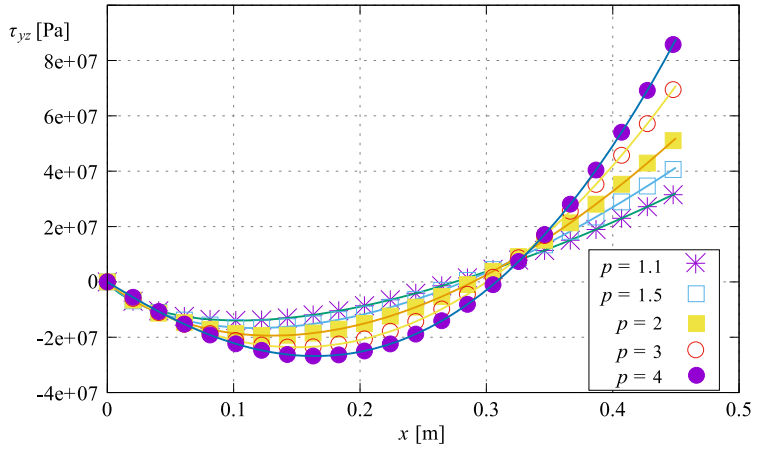

FIG. 3. The plots of shearing stresses $\tau_{yz}(xp)$ as a function of x and p.

The graphs of the function $\tau_{yz}(a, y, p)$ for five different values of p ($p = 1.1$, 1.5, 2, 3, 4) against y are presented in Fig. 4.

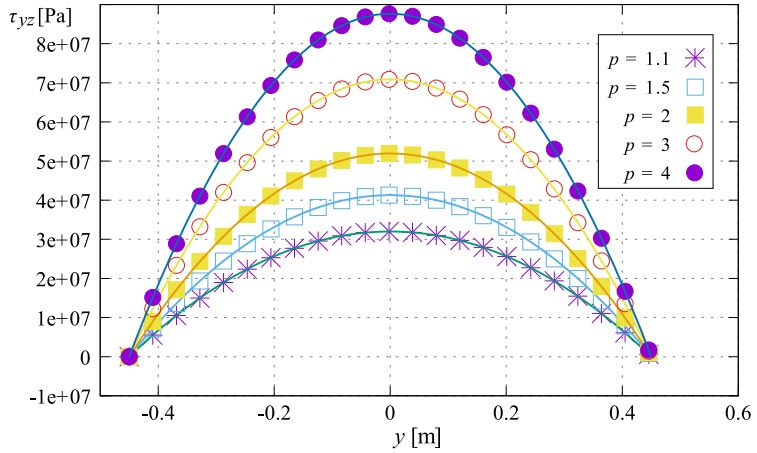

FIG. 4. The plots of shearing stresses $\tau_{yz}(ayp)$ as a function of x and p.

The upper and lower bounds of the torsional rigidity as a function of p are shown in Fig. 5 for $1.01 \leq p \leq 6$.

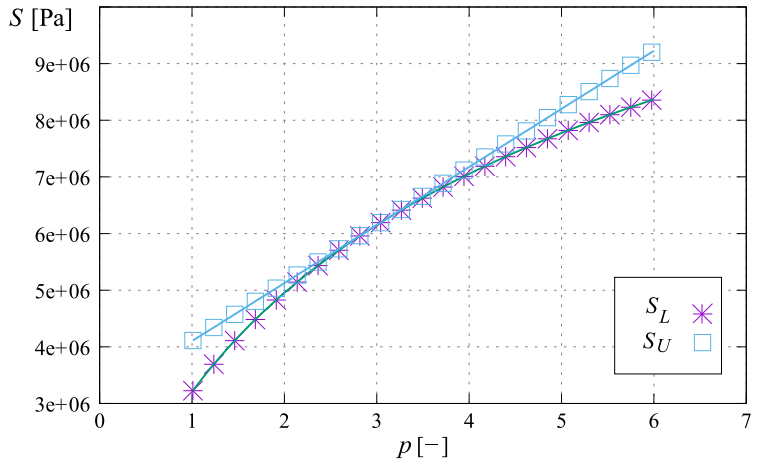

FIG. 5. The plot of S_L and S_U against p.

The comparison of shearing stresses $\tau_{yz}(x, 0, 2)$ and $\tau_{yz}(a, y, 2)$ obtained from the finite element formulation and derived from the approximate analytical solution is shown in Fig. 6.

To compute the finite element solution, the commercial Abaqus software is applied. The numerical model of the problem contains 19 350 C3D20R elements,

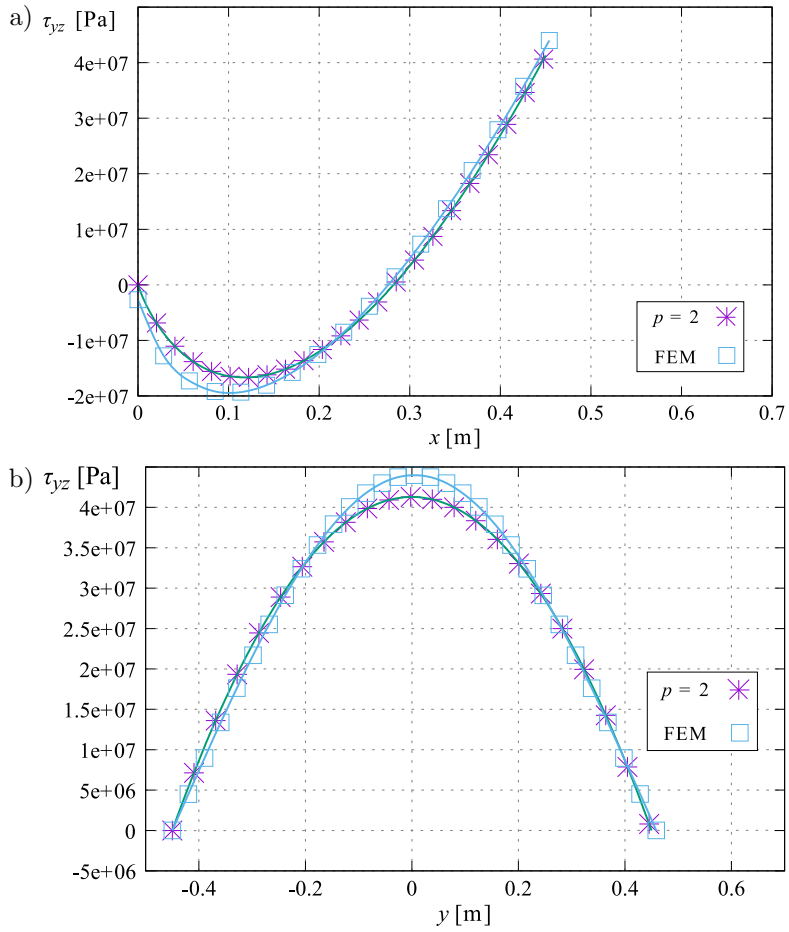

FIG. 6. a) comparison of shearing stresses between FEM and analytical solution $\tau_{yz}(x, 0, 2)$, b) $\tau_{yz}(a, y, 2)$.

which are quadratic three-dimensional continuum elements using reduced integration. The number of unknowns in the model is 251 139.

5. Isotropic isosceles right triangular cross-section

Here, we use the following data:

$$G = G_x = G_y, \qquad \widetilde{U}(x, y) = F_0(x)(y^2 - x^2) \tag{5.1}$$

in Eqs (2.1), (2.2), and (2.3). The function $F_0 = F_0(x)$ satisfies the boundary conditions

$$F_0(a) = 0 \lim_{x \to a} F_0(x) = 0. \tag{5.2}$$

In this case, the solution to the variational problem

$$\max_{U_0(x,y)} \left\{ 4 \int_A U_0\,(x,y)\ \mathrm{d}A - \frac{1}{G} \int_A \left[\left(\frac{\partial U_0}{\partial x} \right)^2 + \left(\frac{\partial U_0}{\partial y} \right)^2 \right] \mathrm{d}A \right\}, \tag{5.3}$$

in the class (5.1) is as follows [18]:

$$U_0(x,y) = \frac{5}{8} G (y^2 - x^2) \ln \frac{x}{a}, \qquad (x,y) \in A \cup \partial A. \tag{5.4}$$

The value of the variational functional (5.3) for this function is [22]:

$$S_{0L} = 0.104\, G a^4. \tag{5.5}$$

Starting from the expression of $S_L(p)$:

$$S_L(p) = \frac{2}{3} G a^4 \frac{4\left(p - \sqrt{6 + 10p}\right)}{(1-p)\left(p + \sqrt{6 + 10p}\right)}, \tag{5.6}$$

it can be proven that

$$\lim_{p \to 1} S_L(p) = S_{0L} = 0.104\, G a^4. \tag{5.7}$$

It should be noted that the exact solution for the isotropic case in the form of an infinite series was given by Leibenzon and he derived the following result for the torsional rigidity [22].

Starting from the expression of the function:

$$S_0 = a^4 \left(\frac{1}{3} - \frac{64}{\pi^5} \sum_{k=1}^{\infty} \frac{1}{k^5} \frac{1 + \cosh(k\pi)}{\sinh(k\pi)} \right) G. \tag{5.8}$$

Assuming $G_x = G_y = G = 5 \cdot 10^7$ Pa, $a = 0.45$ m in the upper and the lower bounds formula for S_0, simple computation gives the following results using Eq. (3.11):

$$S_{0U} = 2.733375 \cdot 10^5\ \mathrm{N} \cdot \mathrm{m}^2, \tag{5.9}$$

$$S_{0L} = S_L(p) = 2.132325 \cdot 10^5\ \mathrm{N} \cdot \mathrm{m}^2, \tag{5.10}$$

$$S_0 = 2.000229 \cdot 10^5\ \mathrm{N} \cdot \mathrm{m}^2. \tag{5.11}$$

Leibenzon's result is in contradiction to the lower bound derived by Lurie and the results achieved in this paper, since

$$S_0 < S_{0L} = S_L(p). \tag{5.12}$$

The authors of this study dealt with the analytical solution of Saint-Venant's torsion of the isotropic bar with a cross-section having an isosceles right-angled triangle. The examined cross-section in the Oxy coordinate system is shown in Fig. 7.

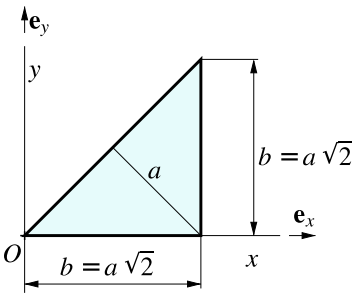

FIG. 7. Isosceles right-angled cross-section.

In this coordinate system, the Prandtl stress function is as follows:

$$U(x,y) = G\,y(x-y) + G\,u(x,y), \tag{5.13}$$

where

$$u(x,y) = \sum_{k=1}^{\infty} c_k \left(\sinh\frac{k\pi}{b}x \sin\frac{k\pi}{b}y - \sin\frac{k\pi}{b}x \sinh\frac{k\pi}{b}y \right), \tag{5.14}$$

and this function must satisfy the following conditions: $\Delta u = 0$ in $(x,y) \in A$ and $u(x,y) = 0$ in $(x,y) \in \partial A$.

The exact value of the torsional rigidity according to Prandtl's formulation of the uniform torsion can be obtained as:

$$S_0 = 2 \int_{x=0}^{b} \int_{y=0}^{x} U(x,y)\mathrm{d}x\,\mathrm{d}y, \qquad b = a\sqrt{2}. \tag{5.15}$$

From formula (5.15) we obtain S as:

$$S = 2.1396775 \cdot 10^5\ \mathrm{N}\cdot\mathrm{m}^2. \tag{5.16}$$

A combination of Eqs. (5.9), (5.10), and (5.16) gives:

$$\begin{aligned} S_{0L} = 2.132325 \cdot 10^5\ \mathrm{N}\cdot\mathrm{m}^2 < S = 2.13967757 \cdot 10^5\ \mathrm{N}\cdot\mathrm{m}^2 \\ < S_{0U} = 2.733375 \cdot 10^5\ \mathrm{N}\cdot\mathrm{m}^2. \end{aligned} \tag{5.17}$$

Figure 8 shows the contour plot of the Prandtl stress function given by Eq. (5.13).

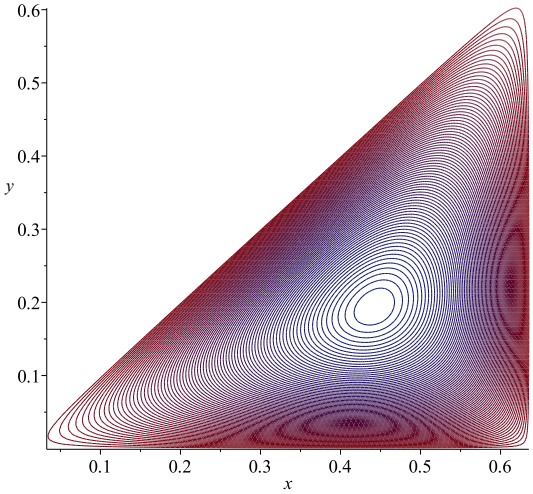

FIG. 8. The contour plot of $U = U(x, y)$.

6. Conclusions

Saint-Venant's torsion of a Cartesian orthotropic bar with isosceles right triangular cross-section was considered in this study. The proposed approximate analytical method, based on the minimum theorem for complementary energy of elasticity, as presented. The paper gives the expression for the Prandtl stress function. Upper and lower bounds are derived for the torsional rigidity. The numerical results in the paper can be used as a benchmark solution to check the accuracy of different numerical methods such as FEM, BEM, finite difference method, etc.

Research in this field continues as scientists and engineers strive to develop more accurate and versatile methods for analyzing the torsional behavior of structures with special cross-sections. Advances in computational methods and materials science contribute to ongoing improvements in the analysis and design of structural components subjected to torsional loads.

References

1. Jog C.S., *Continuum Mechanics. Volume I: Foundations and Applications of Mechanics*, Cambridge University Press, 2015.

2. Sokolnikoff I.S., *Mathematical Theory of Elasticity*, 2nd ed., Robert E. Krieger Publishing Company, Malabar, Florida, 1987.

3. Sparrow E.M., Laminar flow in isosceles triangular ducts, *AIChE Journal*, **8**(5): 599–604, 1962, doi: 10.1002/aic.690080507.

4. Kolossoff M.C., Sur la torsion des primes ayant pour base un triangle rectangle [in French], *Comptes Rendus*, **178**: 2057–2060, 1924.

5. Hay G.E., The method of images applied to the problem of torsion, *Proceedings of the London Mathematical Society*, **s2-45**(1): 382–397, 1939, doi: 10.1112/plms/s2-45.1.382.

6. Leknitskii S.G., *Theory of Elasticity of an Anisotropic Body*, Holden-Day Inc., San Francisco, 1963.

7. Leknitskii S.G., *Torsion of Anisotropic and Non-homogeneous Beams* [in Russian], Nauka, Moscow, 1971.

8. Milne-Thomson L.M., *Antiplane Elastic Systems*, Springer, Berlin, 1962.

9. Sadd M.H., *Elasticity. Theory, Applications and Numerics*, Elsevier, London, 2005.

10. Rand O., Rovenski W., *Analytical Methods in Anisotropic Elasticity with Symbolic Computational Tools*, Birkhäser, Boston, 2005, doi: 10.1007/b138765.

11. Ecsedi I., Baksa A., Saint-Venant torsion of anisotropic bar, *International Journal of Mechanical Engineering Education*, **45**(3): 286–294, 2017, doi: 10.1177/0306419017708642.

12. Ecsedi I., Baksa A., A method for the solution of uniform torsion of Cartesian orthotropic bar, *Journal of Theoretical and Applied Mechanics*, **52**(2): 129–143, 2022, doi: 10.55787/jtams.22.52.2.129.

13. Sarkisian V.S., *Some Problems of the Mathematical Theory of Elasticity of Anisotropic Body* [in Russian], Izd. Erevan University Press, Erevan, 1976.

14. Sarkisian V.S., *Some Problems of Anisotropic Elastic Bodies* [in Russian], Izd. Erevan University Press, Erevan, 1970.

15. Ecsedi I., Baksa A., Estimation of the torsional rigidity of orthotropic solid cross-section, *Engineering Transactions*, **69**(2): 211–221, 2021, doi: 10.24423/EngTrans.1294.20210607.

16. Swider P., Briot J., Estivalézes E., A solution of torsional problem by energy method in the case of anisotropic cross-section, *Archives of Applied Mechanics*, **81**: 801–808, 2011, doi: 10.1007/s00419-010-0450-7.

17. Chen T., Wei C.J., Saint-Venant torsion of anisotropic shafts: Theoretical frameworks, external bounds and affine transformations, *Quarterly Journal of Mechanics and Applied Mathematics*, **58**(2): 269–287, 2005, doi: 10.1093/qjmamj/hbi013.

18. Chen T., A homogeneous elliptical shaft may not warp under torsion, *Acta Mechanica*, **169**(1): 221–224, 2004, doi: 10.1007/s00707-004-0093-2.

19. Ecsedi I., Elliptic cross-section without warping under torsion,*Mechanics Research Communications*, **31**(2): 147–150, 2004, doi: 10.1016/S0093-6413(03)00098-3.

20. Horgan C.O., On the torsion of functionally graded anisotropic linearly elastic bars, *IMA Journal of Applied Mathematics*, **72**(5): 556–562, 2007, doi: 10.1093/imamat/hxm027.

21. Nowinski J.L., Cauchy-Schwarz inequality and the evaluation of torsional rigidity of anisotropic bars, *SIAM Journal of Applied Mathematics*, **24**(3): 324–331, 1973, doi: 10.1137/0124034, https://www.jstor.org/stable/2099768.

22. Lurie A.I., *Theory of Elasticity*, Springer, Berlin, 2005.

Received February 3, 2023; accepted version January 21, 2024.
Online first February 22, 2024.